Appl. Phys. B 72, 611–615 (2001) / Digital Object Identifier (DOI) 10.1007/s003400100554

**Applied Physics B**
Lasers
and Optics

# Nonlinear optical response of Ge nanocrystals in silica matrix with excitation of femtosecond pulses

**H.P. Li[1,*], C.H. Kam[1], Y.L. Lam[1], Y.X. Jie[2], W. Ji[2], A.T.S. Wee[2], C.H.A. Huan[2]**

[1] Photonics Laboratory, School of Electrical and Electronic Engineering, Nanyang Technological University, Nanyang Avenue, Singapore 639798, Republic of Singapore
[2] Department of Physics, National University of Singapore, Lower Kent Ridge Road, Singapore 119260, Republic of Singapore

Received: 21 August 2000/Revised version: 17 January 2001/Published online: 30 March 2001 – 

**Abstract.** We report an investigation of third-order optical nonlinearities in Ge nanocrystals ($\sim 6$ nm radius) embedded in silica matrix using the $Z$-scan and pump-probe techniques with femtosecond laser pulses at 780-nm wavelength. The nanocrystallite Ge samples were prepared using magnetron co-sputtering and post-thermal annealing at 800 °C. The nonlinear absorption coefficient and refractive index of the Ge nanocrystals were determined to be in the range from $1.8 \times 10^{-7}$ to $6.8 \times 10^{-7}$ cm/W and $1.5 \times 10^{-12}$ to $8.0 \times 10^{-12}$ cm$^2$/W, respectively, which are proportional to the Ge atomic fraction in the matrix. Relaxation of the nonlinear response was found to have two characteristic time constants, 1.8 ps and 65 ps. The mechanisms responsible for the observed nonlinear response are discussed.

**PACS:** 42.65.An; 61.46.+w; 78.20.Ci

In recent years there has been considerable interest in the linear and nonlinear optical properties of quantum-confined semiconductor nanocrystals (NCs), particularly for their potential applications in opto-electronics and signal processing. Glass is an attractive host matrix for NCs in such optical applications. In the semiconductor-doped glasses, the energy structure of semiconductor NCs, in particular the energy band gap, can be varied in a broad range by altering the average NC size. Meanwhile, three-dimensional quantum confinement results in discrete energy structures and atomic-like selection rules for interband and intraband optical transitions in semiconductor NCs. Glasses containing semiconductor NCs exhibit interesting optical properties, including tunable absorption, strong photo- and electro-luminescence, and large third-order optical nonlinearities [1–4].

Since the observation of the efficient visible photoluminescence from porous Si [5], nanocrystallite Si and Ge structures have extensively been studied [6] because it would open a new possibility for indirect-gap semiconductors as new materials for opto-electronic applications. In comparison with electronic properties of Si, Ge has a larger dielectric constant and small effective masses for electrons and holes, and the energy difference ($\Delta E = 0.12$ eV) between the indirect gap ($E_g = 0.66$ eV at 300 K, $\Gamma'_{25} \rightarrow L_1$) and the direct gap ($E_0 = 0.8$ eV : $\Gamma'_{25} \rightarrow \Gamma'_2$) is smaller. The exciton Bohr radius of bulk Ge (24.3 nm) [7] is much larger than that of bulk Si (4.9 nm) [8], which implies that the quantum size effects will be more prominent in Ge NCs even for larger size of the crystallites. These electronic conditions lead to an expectation that it is much easier to change the electronic structure around the band gap of Ge, resulting in strong modification of its optical properties. The visible and near-infrared photoluminescence from Ge NCs embedded in silica matrices have been observed [6, 9], which are attributed to the quantum confinement mechanism. The refractive nonlinearity of Ge NCs in a silica matrix fabricated by ion-implantation and annealing has been recently reported [10] using time-resolved degenerate-four-wave-mixing (DFWM) measurements. Strong refractive nonlinearity was observed and relaxation of the nonlinear response was found to have two characteristic time constants: one $< 100$ fs and the other $\sim 1$ ps.

In this paper, we report an experimental investigation of third-order optical nonlinearities of Ge NCs embedded in silica matrix formed by magnetron co-sputtering and annealing using femtosecond laser pulses at 780-nm wavelength. Both the nonlinear absorption coefficient $\beta$ and nonlinear refractive index $n_2$ in the Ge NCs have been measured using the $Z$-scan technique. It has been found that the measured $\beta$ and $n_2$ values range from $1.8 \times 10^{-7}$ to $6.8 \times 10^{-7}$ cm/W and $1.5 \times 10^{-12}$ to $8.0 \times 10^{-12}$ cm$^2$/W, respectively, which are proportional to the Ge atomic fraction in the matrix. We also present femtosecond pump-probe results at 780 nm that allow the determination of the nonlinear response time of the NCs. The mechanisms responsible for the observed nonlinear response are discussed.

## 1 Experimental

The samples employed in this study were nanocomposite films of Ge NCs embedded in silica matrix, which were prepared using magnetron co-sputtering technique in an argon ambient at room temperature with an Anelva (SPF-210H) sputtering system and post-annealed at 800 °C [11]. The films were deposited on double-sided polished fused-

*Corresponding author.
(Fax: +65-791/2687, E-mail: ps2682748e@ntu.edu.sg)

quartz substrates for optical measurements and silicon (100) substrates for high-resolution transmission electron microscope (HRTEM) imaging. The Ge atomic concentration in the films ranges from 8.5% (Sample 1), 12.6% (Sample 2), 14.7% (Sample 3) to 27.6% (Sample 4), which were determined using a VG ESCALAB XPS instrument. The structural characterization of the Ge NCs in the films was made using a Philips CM300 high-resolution transmission electron microscopy (HRTEM) operating at 300 kV. The samples for the HRTEM observation were prepared by standard procedures including mechanical and Ar-ion thinning techniques. The linear optical absorption spectra of the samples were measured by using a Hitachi U-3040 spectrophotometer at room temperature, as compared to the silicon oxide film without Ge doping.

The sensitive and reliable $Z$-scan technique [12] was used to determine the $\beta$ and $n_2$ values of the samples. In our $Z$-scan experiment, the laser pulses at 780-nm wavelength were delivered by a mode-locked Ti:sapphire laser operating at a repetition rate of 76 MHz. The FWHM pulse duration was 150 fs. The spatial profile of the laser beam was of nearly Gaussian distribution after passing through a spatial filter. The minimum beam waist $\omega_0$ of the focused laser beam was measured to be 19 μm. The linearly polarized pulses were divided by a beam-splitter into two parts: the reflected one used as a reference to represent the incident light power; and the transmitted one was focused through the sample. Both the beams were recorded by two power probes (Newport 818 SL) simultaneously, and measured by a dual-channel power meter (Newport 2832-C) which transferred the digitized signals to a computer. The sample was mounted on a computer-controlled translation stage that moved the sample along the $Z$-axis with respect to the focus of the lens. When the nonlinear refraction was measured, a small aperture was placed in front of the transmission detector. As a reference, we performed a $Z$-scan on a sample of polycrystalline ZnSe, and obtained $n_2 = 2.3 \times 10^{-14}\,\mathrm{cm^2/W}$ ($1.0 \times 10^{-11}$ esu) and $\beta = 3.8 \times 10^{-9}\,\mathrm{cm/W}$, which are in good agreement with the published results [13].

All the $Z$-scan measurements on the samples with different Ge concentration were conducted using the above-described $Z$-scan system with different laser irradiances. The thickness of the samples is 1.4 μm, which is much less than the Rayleigh confocal parameter $z_0 = \pi w_0^2/\lambda$ of the Gaussian beam. We also performed open-aperture (OA) and small-aperture (SA) $Z$-scans with different laser polarization directions. No noticeable change in the measurements indicates that the $Z$-scan results are independent of the beam polarization.

The dynamic response of the observed nonlinearity of the samples was examined by a femtosecond pump-probe technique [14]. In the pump-probe experiment, femtosecond pulses at 780-nm wavelength were generated by the same laser source as used in our $Z$-scan measurements. The pump and probe beams with a intensity ratio of 10 : 1 were formed by splitting the beam from the laser output and polarized perpendicularly with respect to each other. The pump beam was chopped at 1.5 kHz and the probe beam was passed through a variable optical delay stage controlled by a computer. The two beams were focused and crossed at a small angle on the sample with a beam-spot size of 28 μm by a lens ($f = 10$ cm). The transmitted probe beam was detected by a photodiode connected with a lock-in amplifier, and the data were sent to the computer. The high stability of the laser and the high-repetition rate of the tunable pulses (76 MHz) permit very high-sensitivity measurements for the changes in the probe transmission $\Delta T/T$.

## 2 Results and discussion

Figure 1a shows the cross-sectional HRTEM image of Sample 3, where those patches represent the Ge NCs. The corresponding size distribution of the Ge NCs was determined as shown in Fig. 1b, which can be well de-

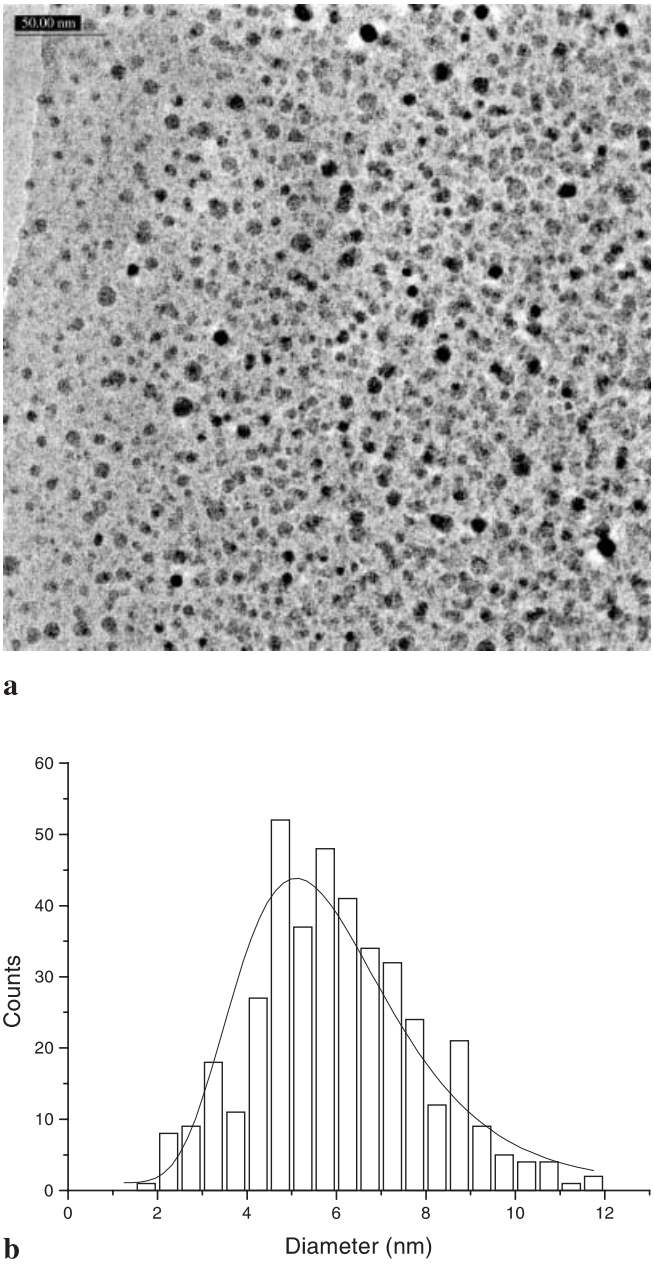


**Fig. 1a,b.** The HRTEM micrography (**a**) and the corresponding size distribution (**b**) for Sample 3. The *solid line* in **b** is a lognormal fit to the size distribution of the NCs. The mean diameter of Ge nanocrystals is $6 \pm 1.8$ nm

scribed by a lognormal function with a geometric mean diameter of 6.0 nm and a dimensionless geometric standard deviation of 1.8 nm. It is obvious that the Ge NCs are nearly uniformly distributed in the thin films. The linear optical absorption spectra of the samples show that all samples exhibit qualitatively similar absorption behavior. Typical linear absorption spectrum for Sample 3 is displayed in Fig. 2, as compared to the spectrum of the silicon-oxide reference film. One can see that the linear absorption of the reference film is negligible in the visible and near-infrared ranges. However, when Ge NCs are present in the film, the spectrum shows two resonant absorption ramps at around 1.2 and 3.0 eV, respectively, which may correspond to the $\Gamma'_{25} \rightarrow \Gamma'_2$ ($\Delta E \sim 0.8$ eV) transitions and transitions $\Gamma'_{25} \rightarrow \Gamma'_{15}$ ($\Delta E \sim 2.7$–$3.6$ eV) in bulk Ge [10]. The linear absorption coefficient $\alpha_0$ of the films is dependent on the Ge NCs' concentration and ranges from $2.1 \times 10^3$ to $6.4 \times 10^3\,\mathrm{cm}^{-1}$ at 780-nm wavelength.

As an example, Fig. 3 shows typical OA and SA $Z$-scans for Sample 3 obtained with linearly polarized 780-nm, 150-fs pulses. Note that all the input irradiances reported here are the peak irradiances at the focus within the samples. We assume that the total absorption coefficient can be written as $\alpha = \alpha_0 + \beta I$, where $I$ is the irradiance of the laser beam within the sample. By applying the OA $Z$-scan theory [12], we numerically calculated the normalized power transmittance as a function of the $z$ position of the sample using $\beta$ as a free parameter. The $\beta$ value can then be extracted from the best fitting. The solid line in Fig. 3a shows the best fit to experimental $Z$-scan data at an irradiance of $0.98\,\mathrm{GW/cm^2}$, which yields that $\beta = 3.8 \times 10^{-7}\,\mathrm{cm/W}$. We also conducted OA $Z$-scan measurements on Sample 3 at the input irradiances ranging from 0.3 to $1.8\,\mathrm{GW/cm^2}$. It was found that the measured $\beta$ value is independent of the laser irradiance (see Fig. 4), which implies the observed nonlinear absorption is of third-order process.

Similarly we express the total refractive index of the sample as $n = n_0 + n_2 I$, where $n_0$ is the linear index of refraction. It should be pointed out that, in our $Z$-scan measurements with high-repetition-rate laser pules, the thermal-lens effect is actually important due to the strong linear absorption in the samples at 780-nm wavelength. Hence, the SA $Z$-scans are

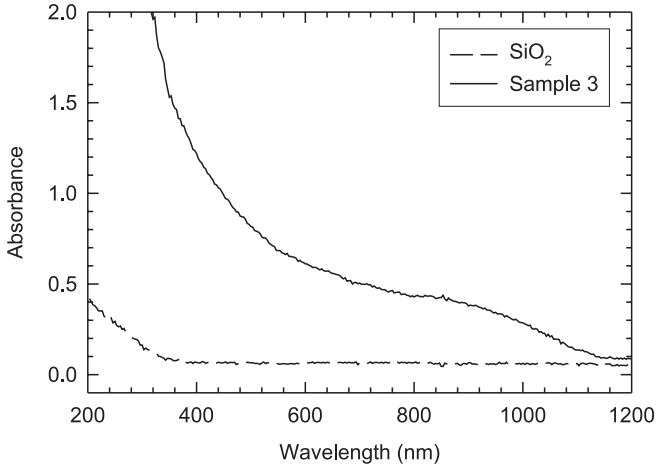


**Fig. 2.** Linear absorption spectra for Sample 3 and the silicon-oxide reference film

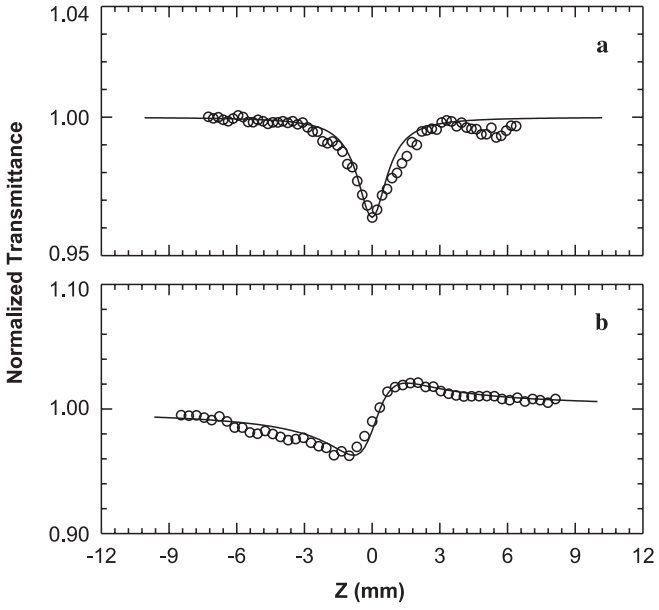


**Fig. 3a,b.** $Z$-scan measurement on Sample 3 at an input irradiance of $0.98\,\mathrm{GW/cm^2}$: **a** open-aperture $Z$-scans, and **b** small-aperture $Z$-scans. The *open circles* are the experimental data. The *solid curves* are the theoretical fits described in the text

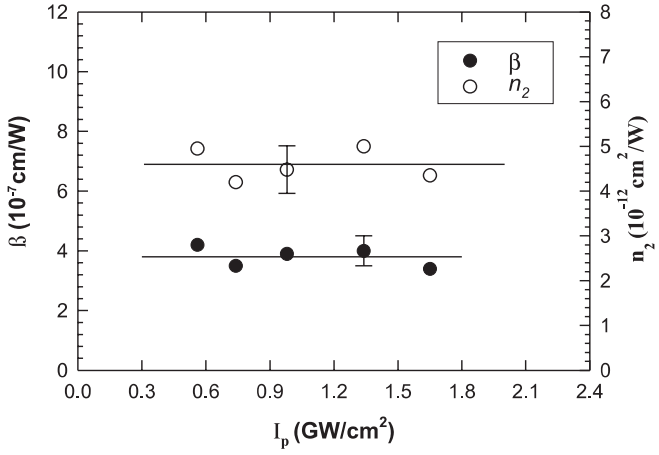


**Fig. 4.** Measured $\beta$ (*full circles*) and $n_2$ (*open circles*) values versus the input irradiance, $I_\mathrm{p}$, for Sample 3. The *solid lines* are guides for the eyes

sensitive to nonlinear refraction of either electronic or thermal origin, and to nonlinear absorption. Yang et al. [15] proposed a thin-lens model to analyze the $Z$-scan measurements with high-repetition-rate pulses. The normalized transmitted power for SA $Z$-scans is given by

$$T = \frac{1}{1+\beta I_0 \left[\frac{1-\exp(-\alpha L)}{\alpha}\right] \Big/ (1+\zeta^2)} \times \left[\frac{C_1 z}{(1+\zeta^2)^2} + \frac{C_2 z}{(1+\zeta^2)} - 1\right]^{-2}, \quad (1)$$

where

$$C_1 = \frac{2LI_0 n_2}{n_0^2 w_0^2}, \quad C_2 = \frac{LP_\mathrm{inc} K_\mathrm{T}}{\pi n_0^2 w_0^2},$$

$\zeta = z/z_0$, $z_0 = \pi w_0^2/\lambda$, $I_0$ is the peak irradiance at the focal plane, $P_{\text{inc}}$ the beam average power on the sample, $L$ the sample thickness, $w_0$ the Gaussian beam radius, and $K_{\text{T}}$ a constant related to the thermo-optic coefficient and thermal conductivity of the film. It should be emphasized that $n_2$ in (1) is the electronic contribution to nonlinear refractive index, excluding the thermal contribution. $C_1$ and $C_2$ represent electronic and thermal contribution to nonlinear phase shift, respectively. The differing $z$ dependence of the two terms with $C_1$ and $C_2$ inside the brace of (1) comes about because the electronic contribution to the refractive nonlinearity is proportional to the peak irradiance, whereas the thermal contribution is proportional to the laser average power. By applying (1), the $n_2$ and $K_{\text{T}}$ values were extracted from the best fits to experimental SA $Z$-scans at five different input irradiances. The obtained value was $n_2 = 4.6 \times 10^{-12}\,\text{cm}^2/\text{W}$, which is independent of the input irradiance up to $1.8\,\text{GW/cm}^2$ (see Fig. 4), implying the observed nonlinear refraction is of Kerr nonlinearity. We also conducted $Z$-scans on the silicon-oxide reference film, and no nonlinearities were measurable. This indicates that the Ge NCs give rise to the observed nonlinearities in the Ge NCs nanocomposite films.

Similar $Z$-scans and analysis procedures have been carried out for the other samples. The measured $\beta$ and $n_2$ values versus the Ge concentration in the films are shown in Fig. 5, which indicates that the $\beta$ and $n_2$ values range from $1.8 \times 10^{-7}$ to $6.8 \times 10^{-7}\,\text{cm/W}$ and $1.5 \times 10^{-12}$ to $8.0 \times 10^{-12}\,\text{cm}^2/\text{W}$, respectively. The results also show that both $\beta$ and $n_2$ increase linearly with the Ge concentration in the films. The obtained $n_2$ values are close to those of the Ge NCs in a silica matrix fabricated by ion implantation and thermal annealing [10] after considering Ge-concentration dependence of $n_2$. The small discrepancy should be expected since our NCs' preparation method is different from the ion implantation.

Figure 6 shows a typical example of time-resolved differential transmission $\Delta T/T$ of the probe beam for Sample 3

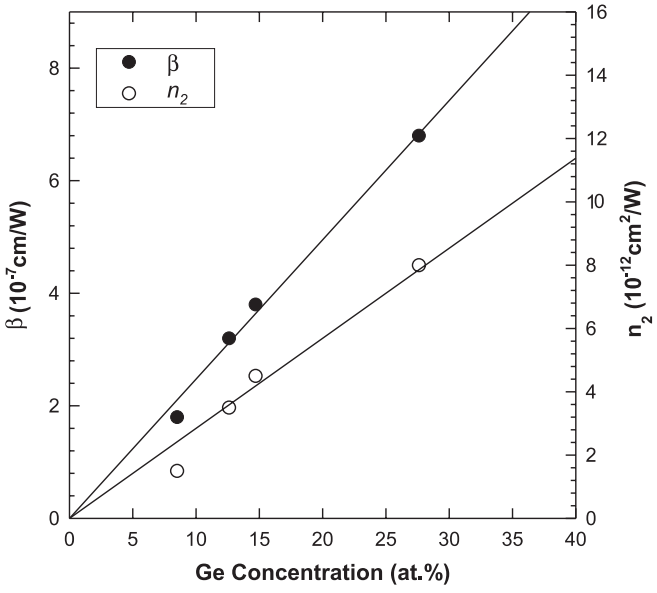


**Fig. 5.** Measured $\beta$ (*full circles*) and $n_2$ (*open circles*) values versus the Ge atomic concentrations in the films

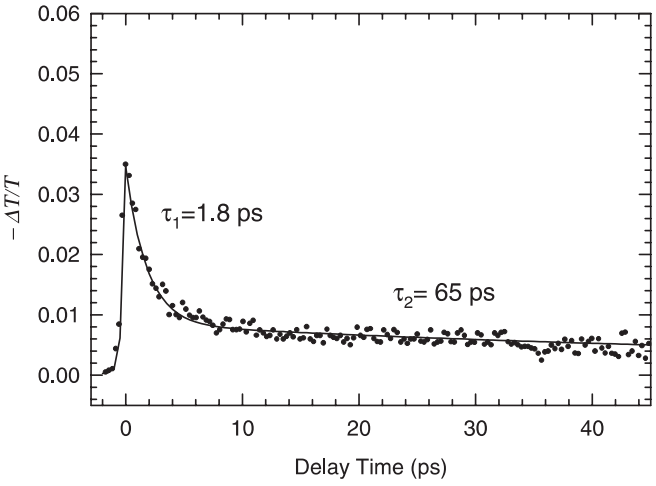


**Fig. 6.** Differential transmission $\Delta T/T$ versus pump-probe delay in Ge NCs (Sample 3). The *solid line* is fit to a double-exponential decay

measured at a pump intensity of $3.3\,\text{GW/cm}^2$. $\Delta T/T$ is negative indicating the characteristic of photo-induced absorption in the Ge NCs films. This is consistent with the results of our OA $Z$-scans. The temporal profile of photo-induced absorption in Fig. 6 shows a two-component decay: initial fast relaxation, followed by a slow decay, which are well described in terms of double-exponential decay with time constants of 1.8 ps and 65 ps.

Ge is an indirect-gap material in the bulk form. In low-dimensional semiconductors, due to confinement-induced mixing of states, optical transitions across originally an indirect energy gap can be allowed in the first order of the perturbation theory. However, calculations performed, e.g. for Si NCs [16, 17], show that the probability of these transitions remains low unless the NC size is smaller than 2–3 nm. Therefore, one can hardly expect a large confinement-induced increase in absorption in case of the relatively large Ge NCs ($\sim 6.0\,\text{nm}$ in diameter) studied in the present experiments. This can explain the absence of sharp features in linear absorption and pronounced bleaching in femtosecond pump-probe measurement.

The nonlinear optical response in indirect-gap semiconductors is dominated by free-carrier absorption due to intraband transitions [18, 19]. The intraband transitions between quantized levels, can be significantly enhanced in quasi-zero-dimensional structures [20], leading to large excited-state absorption. The excited-state absorption due to intraband transitions most likely dominates the nonlinear optical response in Ge NCs. Therefore, the observed photo-induced absorption in Fig. 6 might be assigned to excited-state absorption due to intraband transitions. The two-component decay with time constants 1.8 ps and 65 ps in Fig. 6 may represent two different relaxation processes of the excited carriers. We suppose that the fast 1.8-ps scale may be due to relaxation of excited carrier to the bottom of the conduction band through phonon scattering, which is consistent with the reported intraband transition lifetime in [21, 22], and the slow 65-ps decay may be attributed to carrier trapping at surface-localized defects. We suggest that further investigation is needed such as pump continuum-probe spectroscopy, which is very informative because it provides information on the evolution of the excited carrier distribution function at different energies.

## 3 Conclusion

We have studied the optical nonlinearities of Ge NCs ($\sim 6$ nm radius) embedded silica thin films using $Z$-scan and pump-probe techniques with 780-nm femtosecond pulses. The nonlinear absorption coefficient and refractive index of Ge NCs have been determined to be in the range from $1.8 \times 10^{-7}$ to $6.8 \times 10^{-7}$ cm/W and $1.5 \times 10^{-12}$ to $8.0 \times 10^{-12}$ cm$^2$/W, respectively, and found to be proportional to the Ge NCs' concentration in the films. The nonlinear optical response in Ge NCs shows photo-induced absorption tentatively assigned to excited-state absorption due to intraband transitions, which have been found to have a two-component decay with an initial fast (1.8 ps) relaxation followed by a slow (65 ps) decay.

## References


1. T. Inokuma, Y. Wakayama, T. Muramoto, R. Aoki, Y. Kurata, S. Hasegawa: J. Appl. Phys. **83**, 2228 (1998)
2. S. Vijayalakshmi, M.A. George, H. Grebel: Appl. Phys. Lett. **70**, 708 (1997)
3. N.R. Kulish, V.P. Kunets, M.P. Lisitsa: Superlattices Microstruct. **22**, 341 (1977)
4. E. Vanagas, J. Moniatte, M. Mazilu, P. Riblet, B. Honerlage, S. Juodkazis, F. Paille, J.C. Plenet, J.G. Dumas, J. Vaitkus: J. Appl. Phys. **81**, 2384 (1997)
5. L.T. Canham: Appl. Phys. Lett. **57**, 1046 (1990)
6. S. Takeoka, M. Fujii, S. Hayashi, K. Yamamoto: Phys. Rev. B **58**, 7921 (1998) and references therein
7. Y. Maeda, N. Tsukamoto, Y. Yazawa, Y. Kanemitsu, Y. Masumoto: Appl. Phys. Lett. **59**, 3168 (1991)
8. A.G. Cullis, L.T. Canham, P.D.J. Calcott: J. Appl. Phys. **82**, 909 (1997)
9. Y. Maeda: Phys. Rev. B **51**, 1658 (1995)
10. A. Dowd, R.G. Elliman, M. Samoc, B. Luther-Davies: Appl. Phys. Lett. **74**, 239 (1999)
11. Y.X. Jie, A.T.S. Wee, C.H.A. Alfred, S. P Ng, W.K. Choi: J. Appl. Phys. Lett., submitted
12. M. Sheik-Bahae, A.A. Said, T.H. Wei, D.J. Hagan, E.W. Van Stryland: IEEE J. Quantum Electron. **QE-26**, 760 (1990)
13. T.D. Krauss, F.W. Wise: Appl. Phys. Lett. **65**, 1739 (1994)
14. P. Langot, R. Tommasi, F. Vallee: Phys. Rev. B **54**, 1775 (1996)
15. R.F. Haglund, Jr., L. Yang, R.H. Magruder III, J.E. Wittig, K. Becker, R.A. Zuhr: Opt. Lett. **18**, 373 (1993); L. Yang: Ph.D. Dissertation (Vanderbilt University 1993)
16. G.D. Sanders, Y.-C. Chang: Phys. Rev. B **45**, 9202 (1992)
17. C. Delerue, G. Allan, M. Lannoo: Phys. Rev. B **48**, 11 024 (1993)
18. V.I. Klimov, C.J. Schwarz, D.W. McBranch: Appl. Phys. Lett. **73**, 2603 (1998)
19. V. Grivikas, J. Linnros, A. Vigelis, J. Seckus, J.A. Tellefsen: Solid State Electron. **35**, 299 (1992)
20. V. Milanovic, Z. Ikonic: Phys. Rev. B. **39**, 7982 (1989)
21. V.I. Klimov, C.J. Schwarz, D.W. McBranch, C.A. Leatherdale, M.G. Bawendi: Phys. Rev. B **60**, R2177 (1999)
22. J. Wang, M. Sheik-Bahae, A.A. Said, D.J. Hagan, E.W. Van Stryland: J. Opt. Soc. Am. B **11**, 1009 (1994)